Cyclic Loading Experiments of Concrete Filled Steel Bridge Piers Under High Compressive Axial Force

Kiyoshi Ono[1], Mitsuyoshi Akiyama[2] and Hideki Imanishi[3]

Abstract

Some methods for evaluating the seismic performance of steel bridge piers have been already proposed in the previous investigations. Almost previous studies dealt with steel piers and members subject to relatively low compressive axial force that is below $0.2N_y$, where N_y is a yield axial force. Little is known about the seismic performance of steel members subject to the high compressive axial force. On the other hand, it is reported that the huge earthquakes like the Kobe Earthquake may cause the high compressive axial force to the steel members such as arch ribs and towers of suspension bridges. Therefore, it is very important to grasp the seismic performance of steel members under the high compressive axial force in order to develop the seismic design method of them. In this study, cyclic loading experiments of the concrete filled steel bridge piers were conducted by changing the value of the compressive axial force applied to each test specimen. On the basis of the experimental results, the effect of the compressive axial force on the seismic performance of concrete filled steel bridge piers is investigated.

Introduction

The Kobe Earthquake in 1995 caused the destructive damage to highway bridges like never seen before in Japan. The seismic design specifications for highway bridges were revised in 1996 (Japan Road Association. 1996) in consideration of the damage and the ductility design method, which had already been adapted to reinforced concrete bridge piers, was also introduced to steel bridge piers. And the more detailed seismic design method for steel bridge piers is specified in the 2002 specifications (Japan Road Association. 2002b).

By the way, it is reported that the huge earthquakes like the Kobe Earthquake may cause the high compressive axial force to rigid frame steel piers, arch ribs and towers of suspension bridges by varying axial force and the compressive axial force sometimes exceeds $0.5\ N_y$. Here, N_y represents the yield axial force. However, the previous seismic evaluation methods mentioned above were proposed on the basis of the researches as to steel bridge piers and steel members subject to the low compressive axial force such as $0.2\ N_y$. As for hollow steel members with stiffened rectangular sections under the high

---

[1] Associate Professor, Dept. of Civil Engineering, Osaka University
[2] Associate Professor, Dept. of Civil and Environment Engineering, Tohoku University
[3] Deputy Director, Kinki Regional Development Bureau, Ministry of Land, Infrastructure and Transport

compressive axial force such as 0.5 N_y, the experimental and numerical researches were conducted and the new seismic performance evaluation method is proposed (Okada et al. 2010). On the other hand, studies on seismic performance of the concrete filled steel bridge piers under the high compressive axial force are few and it is little known. Therefore, it is necessary to grasp the seismic performance of concrete filled steel piers under the high compressive axial force for estimating the seismic performance.

In this study, cyclic loading experiments of concrete filled steel piers are conducted by changing the value of the applied compressive axial force. On the basis of the experimental results, the seismic performance of concrete filled steel piers under the high compressive axial force is investigated.

Outline of Experiments

(1) Test Specimens

In this investigation, two test specimens were employed. The dimension, steel grade, and distribution of stiffeners of two test specimens were same although the values of the compressive axial force applied to each specimen were different. The outline of the dimensions of test specimen is given in Figure 1 and the values of the dimensions and the major parameters of the test specimens are listed in Table 1. The figure in the name of each test specimens, '15' of C-15 and '50' of C-50 in Table 1, expresses the percentage of each compressive axial force to the yield axial force, N/N_{yN}. Here, N_{yN} is the yield axial force calculated by the following equation.

$$N_{yN} = \sigma_{yN} \times A \tag{1}$$

Where σ_{yN} = nominal yield stress; A = sectional area of only steel section (excluding the filled concrete).

In Table 1, R_R and R_F are the buckling parameters of plate panels between longitudinal stiffeners and stiffened plate panels respectively. $\bar{\lambda}$ is the slenderness ratio parameter of the pier. The definitions of parameters mentioned above are identical to those stipulated in the 2002 specifications (Japan Road Association. 2002a) and given as follows.

$$R_R = \frac{b}{t} \sqrt{\frac{\sigma_{yM}}{E} \frac{12(1-v^2)}{4\pi^2 n^2}} \tag{2}$$

$$R_F = \frac{b}{t} \sqrt{\frac{\sigma_{yM}}{E} \frac{12(1-v^2)}{\pi^2 k_F}} \tag{3}$$

$$\bar{\lambda} = \frac{1}{\pi} \sqrt{\frac{\sigma_{yM}}{E}} \frac{2h}{r} \tag{4}$$

where h = column height (distance from the bottom of the column to the point of application of horizontal load); r = radius of gyration of cross section of steel members; σ_{yM} = yield stress of steel gained from material experiment; E = Young's modulus of steel; b = flange width; t = plate thickness; v = Poisson's ratio of steel ; n = number of panels; k_R, k_R = bucking coefficient for R_R and R_F respectively.

The steel grade of test specimens was JIS-SM490. In two specimens, the plate thickness of webs, flanges and stiffeners was 6 mm.

(2) Loading Condition

Each test specimen was loaded with hydraulic jacks installed in a fully stiff frame. In respective experiment, the specified compressive axial force as shown in Table 1 was first applied to the test specimen by the vertical hydraulic jack. The values of compressive axial force, N, applied to each test specimen were 15% and 50% of yield axial force, N_{yN}, calculated by the equation (1).

The cyclic loading pattern of the horizontal displacement is schematically shown in Figure 2, where δ_{yN} is calculated by the following equation.

$$P_{yN} = \left(\sigma_{yN} - \frac{N}{A} \right) \frac{Z}{h} \tag{5}$$

$$\delta_{yN} = \frac{P_{yN} h^3}{3EI} \tag{6}$$

where I = moment of inertia of only steel section; Z = section modulus of only steel section.

The axial force was kept constant during the cyclic loading experiments.

Experimental Results and Comments

Figure 3 shows the horizontal load - horizontal displacement relationship (P-δ relationship) and Figure 4 shows the envelope curves gained from the P-δ relationship shown in Figure 3. The square symbols (◆) in Figure 4 show the points where the maximum horizontal load 'P_{max}' was observed.

Furthermore, the envelop curves of hollow steel bridge piers in the previous experimental results (Okada et al. 2010) are shown in Figure 5 in order to compare the seismic performance of the concrete filled steel piers with that of the hollow steel piers. Figure 6 indicates an outline of the test specimens and Table 3 expresses the values of the dimensions, the major buckling parameters, the compressive axial force applied to the test specimens of the hollow steel piers and so on in the previous study. As shown in Tables 1

and 3, the dimensions, the distribution of the stiffeners and the values of some buckling parameters and N/N_{yN} in this study are almost same as those in the previous study although the values of h, $\bar{\lambda}$, γ_l/γ_l^* and σ_{yM} are a little different as for the steel members excluding the filled concrete.

Figures 3 and 4 show that the hysteretic loop size, P_{max} and δ_m decrease with the increase in the applied compressive axial force. Here, δ_m is a horizontal displacement at P_{max}. And the descent of the horizontal load after P_{max} of the test specimen under the high compressive force (C-50) is steeper than that under the low compressive axial force (C-15). The same tendency can be also observed in envelop curves of follow steel piers in Figure 5. From the view point of the comparison between the concrete filled test specimens and the hollow ones under the same value of N/N_{yN}, P_{max} and δ_m of the concrete filled test specimens are lager than those of hollow ones. Furthermore, the descent of envelop curves after P_{max} of the concrete filled test specimens is more gradual than that of hollow ones. Especially, the descent of the envelop curve of C-50 is much more gradual than that of S-50 in comparison of the difference between C-15 and S-15.

Figure 7 shows the strain distribution on the web panel at $+n\delta_{yN}$ until P_{max} as for concrete filled test specimens and Figure 8 shows that of hollow test specimens. Figure 9 indicates the location of the points where strain was measured. According to the comparison between the concrete filled steel piers and the hollow steel piers under the same value of N/N_{yN}, for example, the comparison between Figure 7(a) and Figure 8(a) and that between Figure 7(b) and Figure 8(b), the compressive strain range of the concrete filled test specimen is narrower than that of hollow one. The cause of the narrower compressive strain range in the concrete filled steel piers is that not only the steel section but also the filled concrete bears the compressive stress caused by the compressive axial force and the bending moment and then the burden of the compressive strain on the steel section decreases. And the comparison of the experimental results under the different applied axial force, for instance, the comparison between Figures 7 (a) and (b) and that between Figures 8 (a) and (b), indicates that the compressive strain range of the test specimens under the high compressive axial force is wider than that under the low compressive axial force. The reason for this is that the applied high axial force causes the larger compressive stress and it leads the wider compressive strain range. Regarding the strength of steel members, the wider compressive strain range or the high compressive strain leads the decrease in the ultimate strength of them because bucking is easier to occur under such condition. As shown in Figure 8(b), almost part of the web panel of S-50 corresponds to the compressive strain area while the width in the compressive strain area is below one-third of the web panels as for the other three test specimens including C-50, which is a concrete filled test specimen under the high compressive axial force. It is thought that this difference in the strain distribution in S-50 may lead the very steep descent of the horizontal load after P_{max} and the decrease in P_{max} and δ_m.

Conclusions

Cyclic loading experiments were conducted by changing the value of the compressive axial force applied to concrete filled test specimens in order to gasp the effect of the compressive axial force on seismic performance of the concrete filled steel piers. The results from experiments are concluded as follows.

1) The increase in the compressive axial force causes the decrease in the hysteretic loop size, the maximum horizontal load and the horizontal displacement at the maximum horizontal load and it makes the slope of envelop curves after the maximum horizontal load steep. The feature of seismic performance mentioned above is the same as that of hollow steel piers.

2) The compressive strain range on the steel section of concrete filled steel piers is narrower than that of non-concrete filled steel piers and it is thought that this narrower compressive strain range may lead the increase in the seismic performance.

References

Japan Road Association (1996). *Specifications for highway bridges, Part V: Seismic Design*.

Japan Road Association (2002a). *Specifications for highway bridges, Part II: Steel bridges*.

Japan Road Association (2002b). *Specifications for highway bridges, Part V: Seismic Design*.

Public Works Research Institute of the Ministry of Construction and five other organizations (1997-1999). "Ultimate Limit State Design Method of Highway Bridges Piers under Seismic Loading", *Cooperative Research Report* (in Japanese).

Seiji OKADA, Kiyoshi ONO, Hiroaki TANIUE, Munemasa TOKUNAGA and Nobuo NISHIMURA (2010). "SEISMIC PERFORMANCE OF STIFFENED STEEL MEMBERS WITH RECTANGULAR SECTION UNDER HIGH COMPRESSIVE AXIAL FORCE", *Doboku Gakkai Ronbunshuu A*, Vol. 66, No. 4 (in Japanese).
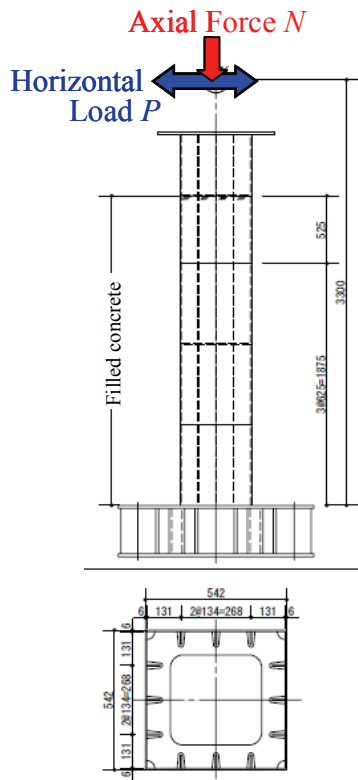
Figure 1 Test specimen

Table 1 Dimensions and parameters of test specimens

|		C-15	C-50
N/N_{yN} (%)		15	50
The size of cross-section (mm)		542 X 542	542 X 542
Thickness of flange plate t_F (mm)		6	6
Thickness of web plate t_W (mm)		6	6
The size of longitudinal stiffener (mm)		53 X 6	53 X 6
The number of stiffeners on flange		3	3
The number of stiffeners on web		3	3
Compressive Axial Force (kN)		786	3,300
The height of Loading point h (mm)		3,300	3,300
Steel grade (JIS)		SM490A	SM490A
γ/γ^*		0.97	0.97
Parameters calculated by nominal yield stress σ_{yN}	$\bar{\lambda}_N$	0.39	0.39
	R_{RN}	0.46	0.46
	R_{FN}	0.47	0.47
Parameters calculated by experimental yield stress σ_{yM}	σ_{yM} (MPa)	381	378
	$\bar{\lambda}_M$	0.43	0.43
	R_{RM}	0.51	0.51
	R_{FM}	0.52	0.51
Height of filled concrete h_c (mm)		2400	2400
Strength of concrete σ_c (MPa)		25.8	25.6
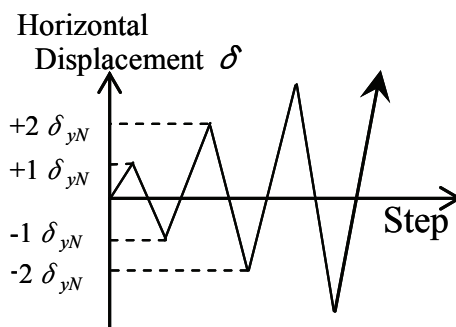
Figure 2 Cyclic loading patterns
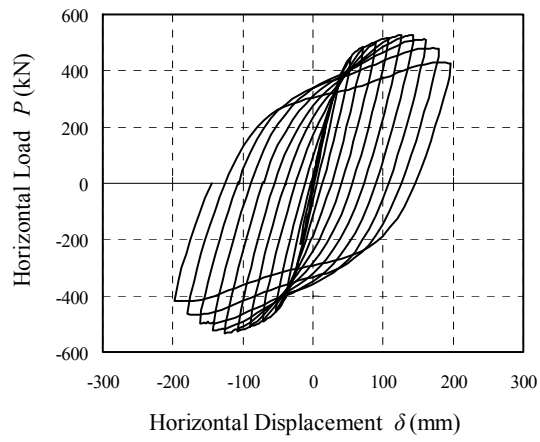
(a) C-15
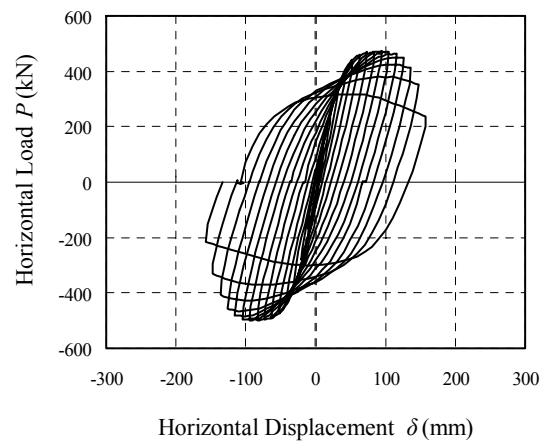
(b) C-50
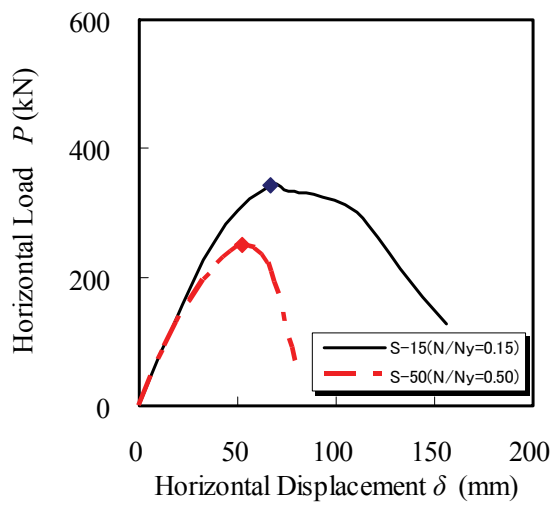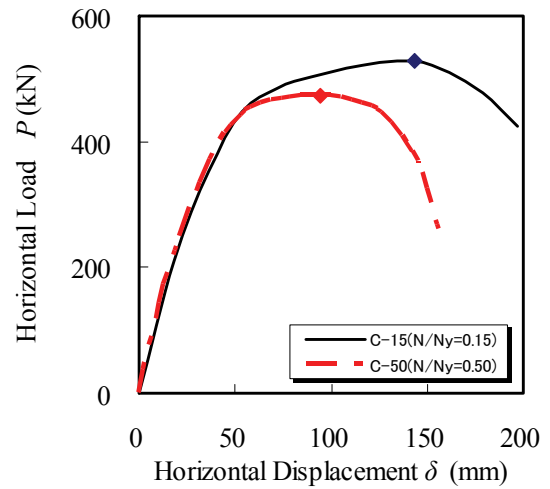
Figure 3 *P-δ* relationship

Figure 4 Envelop curves

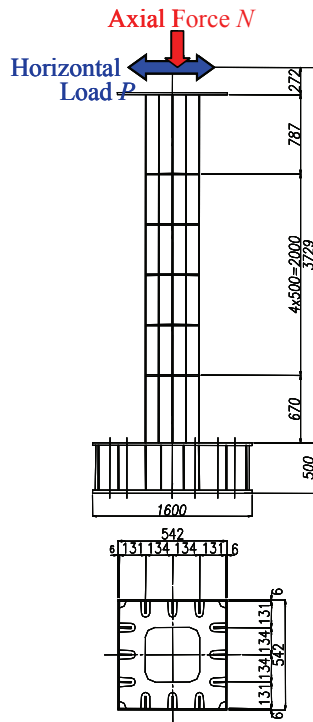**Figure 5 Envelop curves in previous study (Hollow steel piers)**

Figure 6 Test specimen in previous study
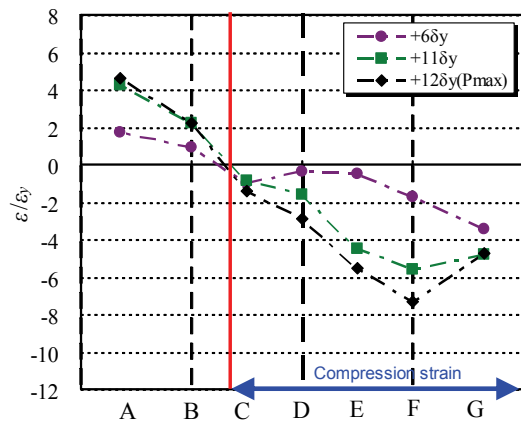
Table 3 Dimensions and parameters of test specimens in the previous study

		S-15	S-50
N/N_{yN} (%)		15	50
The size of cross-section (mm)		542 X 542	542 X 542
Thickness of flange plate t_F (mm)		6	6
Thickness of web plate t_W (mm)		6	6
The size of longitudinal stiffener (mm)		60 X 6	60 X 6
The number of stiffeners on flange		3	3
The number of stiffeners on web		3	3
Compressive Axial Force (kN)		808	2,694
The height of Loading point h (mm)		3,729	3,729
Steel grade (JIS)		SM490A	SM490A
γ/γ^*		1.19	1.19
Parameters calculated by nominal yield stress σ_{yN}	$\bar{\lambda}_N$	0.44	0.44
	R_{RN}	0.45	0.45
	R_{FN}	0.42	0.42
Parameters calculated by experimental yield stress σ_{yM}	σ_{yM} (MPa)	415	418
	$\bar{\lambda}_M$	0.51	0.52
	R_{RM}	0.53	0.53
	R_{FM}	0.49	0.49

(a) C-15

(b) C-50

Figure 7 Strain distribution in web panels of concrete filled test specimens

(a) S-15   **(b) S-50**
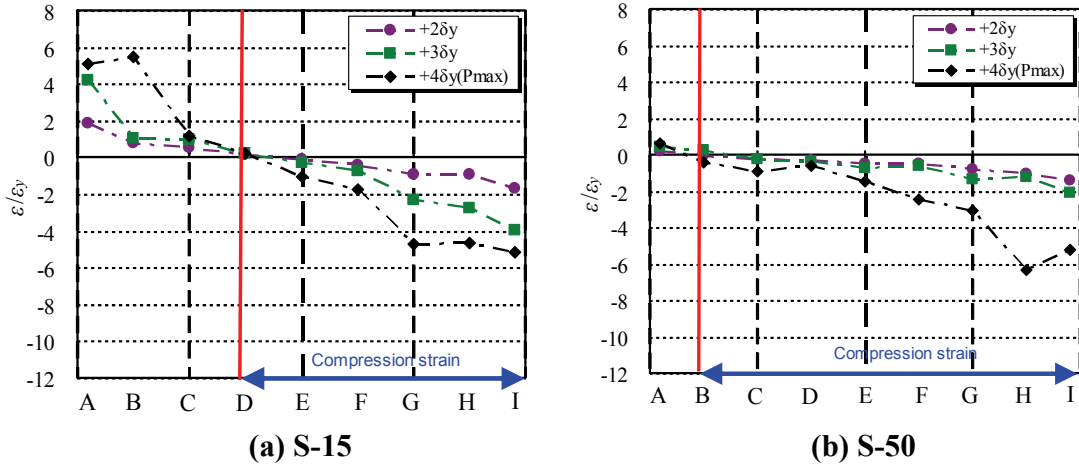
Figure 8 Strrain distribution in web panels of follow test specimens
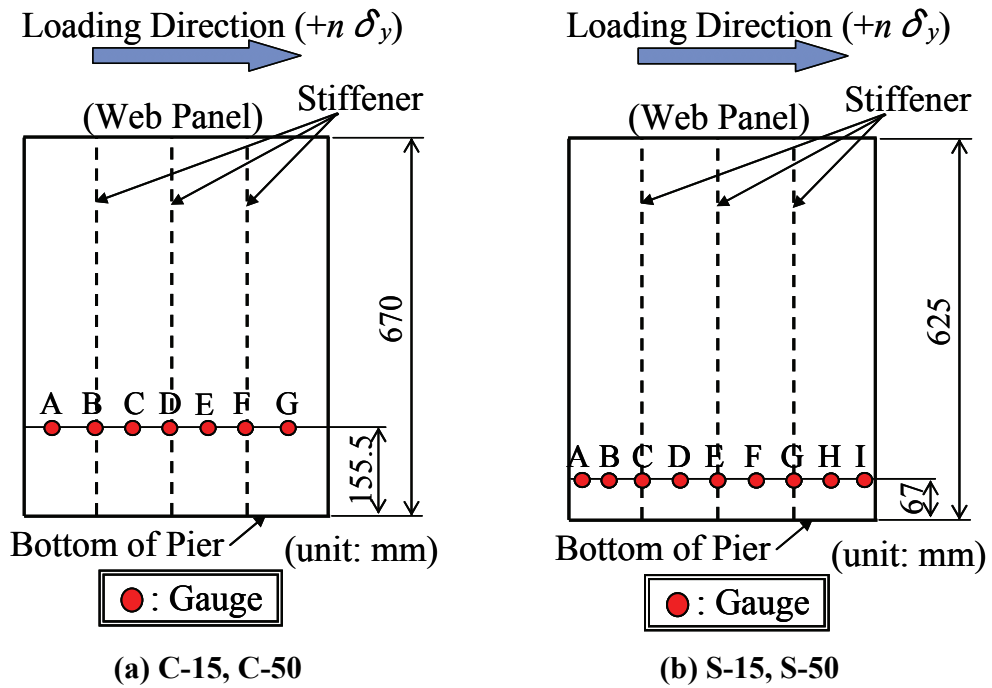

(a) C-15, C-50   **(b) S-15, S-50**

Figure 9 Location of strain gauges on web panels